C. R. Physique 12 (2011) 132–140

Contents lists available at ScienceDirect

Comptes Rendus Physique

www.sciencedirect.com

Propagation and plasmas: new challenges, new applications

Observation and theoretical modeling of electron scale solar wind turbulence

Observations et modélisation théorique de la turbulence à l'échelle électronique dans le vent solaire

Fouad Sahraoui [a,*], Melvyn L. Goldstein [b], K. Abdul-Kader [a], Gérard Belmont [a], Laurence Rezeau [a,c], Patrick Robert [a], Patrick Canu [a]

[a] *Laboratoire de Physique des Plasmas, CNRS-École Polytechnique, Observatoire de Saint-Maur, 4, avenue de Nepture, 94107 Saint-Maur-des-Fossés, France*
[b] *NASA Goddard Space Flight Center, Code 673, Greenbelt, MD 20771, USA*
[c] *Université Pierre-et-Marie-Curie, 4, place Jussieu, 75005 Paris, France*

A R T I C L E I N F O

Keywords:
Solar wind
Turbulence
Dissipation
Cluster
Heating
k-Filtering

Mots-clés :
Vent solaire
Turbulence
Dissipation
Cluster
Chauffage

A B S T R A C T

Turbulence at MagnetoHydroDynamics (MHD) scales in the solar wind has been studied for more than three decades, using data analysis, theoretical and numerical modeling. However, smaller scales have not been explored until very recently. Here, we review recent results on the first observation of cascade and dissipation of the solar wind turbulence at the electron scales. Thanks to the high resolution magnetic and electric field data of the Cluster spacecraft, we computed the spectra of turbulence up to ~ 100 Hz (in the spacecraft reference frame) and found evidence of energy dissipation around the Doppler-shifted electron gyroscale f_{ρ_e}. Before its dissipation, the energy is shown to undergo two cascades: a Kolmogorov-like cascade with a scaling $f^{-1.6}$ above the proton gyroscale, and a new $f^{-2.3}$ cascade at the sub-proton and electron gyroscales. Above f_{ρ_e} the spectrum has a steeper power law $\sim f^{-4.1}$ down to the noise level of the instrument. Solving numerically the linear Maxwell–Vlasov equations combined with recent theoretical predictions of the Gyro-Kinetic theory, we show that the present results are consistent with a scenario of a quasi-two-dimensional cascade into Kinetic Alfvén modes (KAW). New analyses of other data sets, where the Cluster separation (of about ~ 200 km) allowed us to explore the sub-proton scales using the *k*-filtering technique, and to confirm the 2D nature of the turbulence at those scales.

R É S U M É

La turbulence aux échelles magnétohydrodynamique (MHD) dans le vent solaire a été étudiée pendant plus de trois décennies, au moyen d'analyses de données, de modélisations théoriques et de simulations numériques. Cependant, les plus petites échelles n'ont pas été explorées jusqu'à très récemment. Ici, nous passons en revue les résultats récents sur la cascade et la dissipation de la turbulence du vent solaire à l'échelle des électrons. Grâce aux données à haute résolution temporelle des champs magnétique et électrique des satellites Cluster, nous avons obtenu les spectres de la turbulence jusqu'à 100 Hz (dans le référentiel du satellite) et avons mis en évidence une zone de dissipation d'énergie

* Corresponding author.
E-mail address: fouad.sahraoui@lpp.polytechnique.fr (F. Sahraoui).

1631-0705/$ – see front matter
doi:10.1016/j.crhy.2010.11.008

autour de la fréquence $f\rho_e$ correspondant à l'échelle de giration des électrons. Avant sa dissipation, l'énergie subit deux cascades: une cascade classique à la Kolmogorov avec une loi d'échelle $f^{-1.6}$ en dessus de l'échelle de giration des protons, et une nouvelle cascade en $f^{-2.3}$ aux échelles sub-protoniques jusqu'à l' échelle électronique. Au-dessus $f\rho_e$ le spectre a une loi de puissance plus pentue en $f^{-4.1}$ jusqu'à la limite d'observation donnée par le niveau de bruit de l'instrument. La résolution numérique des équations linéaires de Maxwell–Vlasov combinées aux récentes prédictions de la théorique Gyrocinétique, montrent que ces résultats sont conformes à un scénario de cascade quasi-2D suivant le mode d'Alfvén cinétique (KAW). Une analyse plus récente d'un autre jeu de données, où les séparations de cluster étaient de ~ 200 km, nous a permis d'explorer les échelles sous-proton en utilisant la technique *k*-filtering, et de confirmer la nature quasi-2D de la turbulence à ces échelles-là.

1. Introduction

Over the past three decades, the solar wind (SW) has provided a unique "laboratory" to explore fundamentals of the plasma physics in general and turbulence in particular. Owing to the permanent plasma flow ejected by the solar corona, the solar wind shows fluctuations on all physical quantities (magnetic and electric fields, density, temperature, ...) and on all scales. Away form the Sun, the turbulence develops nearly freely from any boundary and evolves under the sole nonlinear interactions taking place within the plasma. This makes the solar wind an ideal place to explore plasma turbulence, theoretically, numerically and observationally. Observations of the SW turbulence have been possible thanks in particular to the availability of the in situ data measured by single spacecraft such as Voyager, Ulysses, and Wind, or multi-satellites like Cluster [1] and Themis. Mono-satellite data allow one to measure fluctuations only in the (temporal) angular frequency domain, while theories of turbulence predict generally (spatial) wave number properties. In the solar wind comparisons between observations and theories is made possible using the frozen-in flow approximation, known also as the Taylor hypothesis, $\omega_{sc} \sim \mathbf{k}.\mathbf{V}_f$, where ω_{sc} is the measured angular frequency in the spacecraft frame and $\mathbf{V}_f$ is the average flow speed. The solar wind being super-sonic and super-Alfvénic, this assumption is justified since all the characteristic low frequency (Alfvén and magnetosonic) waves have phase speeds smaller than V_f. However, the Taylor assumption is violated if high frequency waves, e.g., whistlers are present. It is also violated in other physical contexts, such as the magnetosphere, where all the characteristic speeds (V_f, V_A, C_S) are of the same order. It is worth noticing that even when the Taylor hypothesis is fully justified, one can infer the wave number properties only along the flow direction. The two other directions of space remain unresolved unless further assumption are introduced such as the isotropy of the turbulence. To fully solve the problem of the 3D determination of the properties of the SW, multi-spacecraft data, such as Cluster, and Themis are required.

Early observations of SW turbulence have emphasized magnetohydrodynamic (MHD) scales where the Kolmogorov scaling $k^{-5/3}$ is frequently observed [2], and usually explained by the energy cascade of nonlinearly interacting (inward and outward) Alfvén waves. This *k*-spectrum has been obtained so far using the Taylor hypothesis. Recently, and thanks to the availability of the Cluster multi-spacecraft data, and to the use of multi-point measurements techniques such as the *k*-filtering (known also as the *wave-telescope* technique), new results on the actual 3D turbulence of MHD turbulence are being obtained [3,4]. Here we focus only on the turbulence at frequencies above the proton gyrofrequency ($f_{cp} \sim 0.1$ Hz). Above f_{cp} and up to 10 Hz steeper power law spectra $f^{-\alpha}$ with $2 < \alpha < 4$ have been observed [5–8] and a debate exists as to whether the turbulence has become dispersive following the whistler mode or the KAW branch, before it is dissipated at small scales [9,10].

There are several theoretical predictions on small scale turbulence: Biskamp et al. [11] predicted a $k^{-7/3}$ magnetic spectrum of whistler turbulence either by dimensional analyses *à la Kolmogorov* or numerical simulations. Later on, several authors have confirmed those predictions [12,13]. Recently, Galtier [14] has shown that the exact Yaglom's-type of equations he obtained for isotropic incompressible Hall-MHD (HMHD) turbulence allow one to derive the $k^{-7/3}$ scaling, which provides thus a stronger theoretical ground for the $k^{-7/3}$ spectrum. Weak turbulence theory of anisotropic incompressible HMHD predicts a $k_\perp^{-5/2}$ scaling for either the whistler or the Alfvén branches [12,14,15]. While all these fluid models are good approximations and provide important features of the SW turbulence, one has however to bear in mind their validity limits and the approximations that had been used to derive them from the exact kinetic theory. Such cautions are particularly required in studies of hot plasmas at scales where dissipations occur (e.g., proton or electron gyroscales). For such problems a kinetic theory is needed. But owing to the fact that a turbulence theory in the full-kinetic approximation is yet out-of-reach, simplified kinetic models may provide an alternative. Such theories exist, and one of them is Gyro-Kinetics (GK). This theory has been developed in the seventies for studying confinement in fusion plasmas. It has been introduced only recently into space and astrophysical applications (see [16] where a review of the theory is given). By averaging over the fast motion of protons GK theory allows one to describe only the very slow dynamics of the plasma ($\omega \ll \omega_{cp}$). It assumes furthermore a strong anisotropy $k_\parallel \ll k_\perp$, allowing expansion of the equations on the small parameter $\epsilon = k_\parallel/k_\perp$, making thus the theory mathematically tractable. Under these approximations, the classical fast (or whistler) mode is obviously ruled out. But, GK catches most of the physics of the Alfvén mode ($\omega \sim k_\parallel V_A$) and that of the entropy mode ($\omega = 0$)

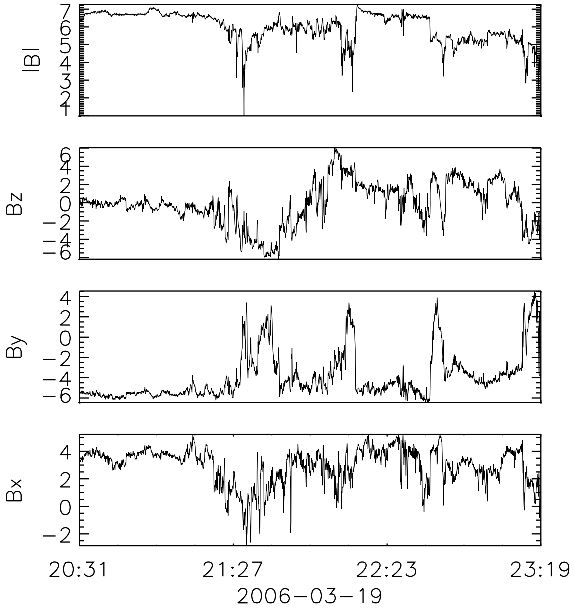

Fig. 1. FGM magnetic field data measured by Cluster 2 in the solar wind plotted in the Geocentric Solar Ecliptic (GSE) reference frame.

down to the electron scales ($k\rho_e \sim 1$). For the scales $1/\rho_e < L < 1/\rho_i$, among others, KG predicts the scalings $k_\perp^{-7/3}$ for the magnetic spectrum and $k_\perp^{-1/3}$ for the electric field spectrum [16,17].

2. High frequency Cluster data in the solar wind

In the present work, we analyze high frequencies (up to 100 Hz) of solar wind magnetic and electric turbulence by taking advantage of high resolution wave data from the Cluster spacecraft [1]. Magnetic data are from the Flux Gate Magnetometer (FGM) and the STAFF-Search Coil (SC) [18,19] experiments, and electric field data are from the Electric Field and Wave experiment (EFW) [20]. FGM data cover the frequency spectrum up to a few Hz. STAFF-SC and EFW provide higher resolution data with two possible sampling rates: 25 Hz (normal mode) and 450 Hz (burst mode). The data used here are burst mode. Due to the small level of the magnetic turbulence in the SW at these very high frequencies, particular attention has been paid to several instrumental issues, in particular, the sensitivity of the STAFF-SC magnetometer. Because of the low sensitivity of the SC sensor at very low frequency, the lowest part of the STAFF-SC spectra has to be filtered. The cut-off frequency can be set to 0.35 Hz on the two perpendicular components to the spin axis. However, in this study, we filtered the spectra at 1.5 Hz to avoid any residual spin effect.

The waveforms shown on Fig. 1 were recorded on 19 March 2006 from 20h32 to 23h20 UT in the solar wind at 1 AU. During this period the Interplanetary Magnetic Field (IMF) was $B \sim 6$ nT, the plasma density $n_p \sim 3\ \text{cm}^{-3}$, the proton and electron temperatures $T_p \sim 50$ eV and $T_e \sim 12$ eV, respectively, the plasma betas (ratios between thermal and magnetic pressures) $\beta_p \sim 2.5$ and $\beta_e \sim 0.7$, respectively for protons and electrons, the plasma velocity $v \sim 640$ km/s, the Alfvén speed $V_A \sim 65$ km/s and the proton gyrofrequency $f_{cp} \sim 0.1$ Hz. The plasma data (protons and electrons) have been obtained from the CIS and the PEACE experiments [1].

Fig. 1 shows the magnetic field components measured by FGM. Note the rotations of B_y coincident with a minimum in the magnetic field magnitude, indicating possible multiple current sheet crossings as the spacecraft move from solar wind toward the bow shock. During this event reflected electrons from the bow shock have been observed both from the Peace and Whisper data.

Fig. 2 shows the power spectra of the magnetic field data from FGM and STAFF-SC, decomposed into the parallel and the perpendicular directions with respect to the mean IMF (defined by averaging over the time interval of Fig. 1). These spectra are calculated using a windowed Fourier transform, where a $\cos^3$ window (having 10% width of the whole interval) is slid to span the time series containing 4×10^6 samples. The spectra shown are the result of averaging all the windows.

Fig. 2 illustrates the good matching between the STAFF-SC and the FGM spectra at frequencies around 1.5 Hz. However, above $f \geqslant 2.5$ Hz, the power in the physical signal falls below the noise floor of the instrument, so we use STAFF-SC data to analyze frequencies above $f \geqslant 2.5$ Hz. Here we merge the low frequency FGM data with the STAFF-SC data at $f = 1.5$ Hz. Fig. 2 shows a spectral breakpoint at $f \sim 0.4$ Hz where the scaling changes from a Kolmogorov spectrum $f^{-1.62}$ to $f^{-2.5}$. Similar breakpoints and steep spectra have been reported previously [5,6,21,8,22], but mostly attributed to energy dissipation [5,6]. The spectra of Fig. 2 suggest rather a very different scenario: the magnetic energy continues cascading for about two decades higher in spacecraft frequency and smaller spatial scales. Furthermore, it shows the first evidence of a

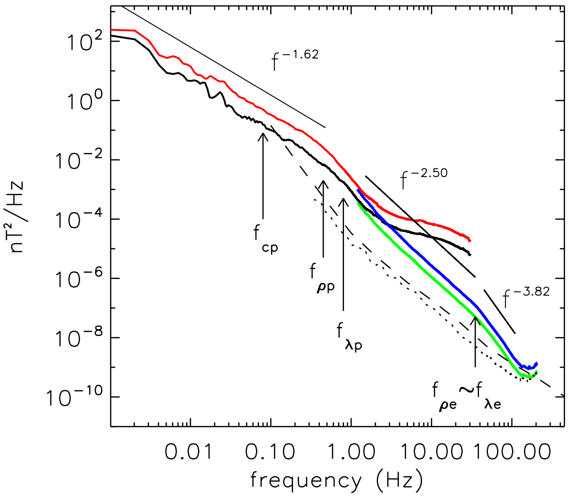

Fig. 2. The parallel (black) and perpendicular (red) magnetic spectra of FGM data ($f < 33$ Hz) and STAFF-SC data (respectively, green and blue; $1.5 < f < 225$ Hz). The STAFF-SC noise level as measured in the laboratory and in-flight are plotted as dashed and dotted lines, respectively. The straight black lines are power law fits to the spectra. The arrows indicate characteristic frequencies defined in the text.

second breakpoint at $f \sim 35$ Hz, followed by a steeper spectrum of $\sim f^{-3.8}$. [23] confirmed these results on several data sets, but they fitted the spectra near the second breakpoint by an exponential law instead of a power law. We emphasize however that those fits concerned not the spectra as measured in the SW but rather the spectra resulting after substracting an estimated sensitivity floor of the Cluster search coils.

To understand the origin of these breakpoints, we calculated the characteristic scales of the plasma, namely the proton and electron gyroscales and inertial lengths defined as $\rho_{p,e} = V_{th_{p,e}}/\omega_{cp,e}$, $\lambda_{p,e} = V_{A_{p,e}}/\omega_{cp,e}$, where V_{th} and V_A are the thermal and the Alfvén velocities, and $\omega_{cp,e}$ are the proton and electron gyrofrequencies. Using the Taylor frozen-in-flow hypothesis ($\omega \sim kv$) these scales are Doppler-shifted and represented in Fig. 2. The Doppler-shifted proton and electron gyroscales fit better with the observed breakpoints than do the proton and electron gyrofrequencies (as has been suggested by [6,8]). In particular, the ratio of the two frequencies $35/0.4 \sim 90$ is very close to the ratio $\rho_p/\rho_e = \sqrt{m_p T_p/m_e T_e} \sim 95$.

The new breakpoint occurs at the electron gyroscale ρ_e, which is very close to λ_e (because $\beta_e \sim 1$). This can be seen clearly on Fig. 3, which shows the high frequency part of two spectra calculated from sub-intervals of Fig. 1 to investigate whether the foreshock electrons have a significant impact on the properties of the observed spectra. Spectra of Fig. 3(a) were obtained in an interval where electron foreshock were detected, whereas those of Fig. 3(b) were calculated when no significant reflected electron were observed from the Whisper data (not shown here). Both spectra look very similar to those of Fig. 2. This is not surprising since the population of electron foreshock represented only a few percents of the total SW electrons. Moreover, if the reflected electrons were to have any impact on the spectra, then this would result in strong spikes on the spectra at electrons scales/frequencies (as these electrons would inject additional energy into the turbulence). Here we observe rather a formation of steep dissipation-like spectrum.

To investigate the nature of the small scale turbulence (i.e., above f_{ρ_p}) we computed the spectrum of the electric field component E_y (shown in Fig. 4). Below f_{ρ_p} the spectrum of E_y shows a high correlation with the spectrum of B_z, and both follow a Kolmogorov scaling. For frequencies around f_{ρ_p} the E_y spectrum steepens slightly up to $f \sim 1.5$ Hz, where it becomes essentially flat. A fit of the spectrum in the interval $f \sim [1.5, 15]$ Hz shows a power law $\sim f^{-0.3}$. It is worth recalling here that GK theories predict the power laws $k_\perp^{-7/3}$ for the magnetic field spectrum and $k_\perp^{-1/3}$ for the electric field spectrum at these sub-proton gyroscales [16,17]. The fact that the electric field spectrum continues with a nearly zero spectral slope above $f \geqslant 10$ Hz is due to reaching the noise level of the EFW experiment.

The present observations suggest that the energy of the turbulence is only slightly damped at the proton gyroscale ρ_p and undergoes another dispersive cascade with the scaling $f^{-2.3}$. Any strong damping would have led to a much steeper spectrum, if not to a clear cut-off [9]. Steepening of spectra (e.g., from $k^{-5/3}$ to $k^{-7/3}$) below the proton scale can indeed be explained solely by dispersive effects as has been predicted by various non-dissipative dispersive MHD models [11,14,12,24]. However, as we show below, finite dissipation may occur at the proton scale ρ_p along with more significant damping at the electron gyroscale ρ_e. This latter may explain the stronger steepening of the spectrum to f^{-4} (the power law fits in the dissipation range may be not very accurate because they extended over less than a decade due to the noise level of the instrument).

3. Theoretical interpretation: Quasi-2D KAW turbulence cascade

This scenario of dispersive cascade and dissipation at electron scales appears consistent with Kinetic Alfvén Wave (KAW) turbulence as predicted by the GK theory [16,17]. The predicted scalings $B^2 \sim k_\perp^{-7/3}$ and $E^2 \sim k_\perp^{-1/3}$ are in striking agree-

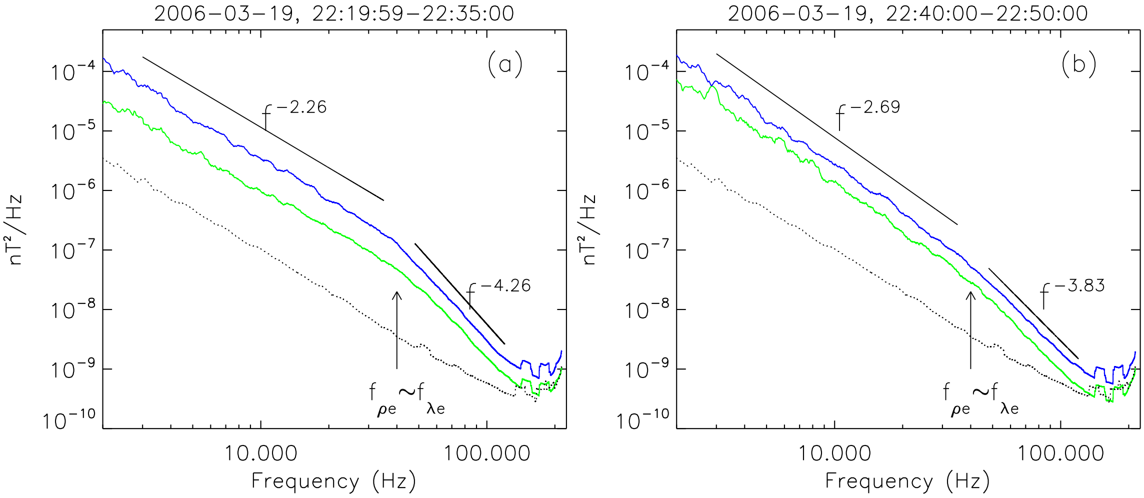

Fig. 3. High-pass filtered power spectra of the parallel (green) and perpendicular (blue) magnetic fluctuations measured by STAFF-SC during two time subintervals with beams of reflected electrons from the bow shock (a) and a nearly free solar wind (no significant reflected electrons) (b). Dotted line is the STAFF-SC noise level. The straight black lines are direct power law fits of the spectra. Vertical arrows are defined in the text.

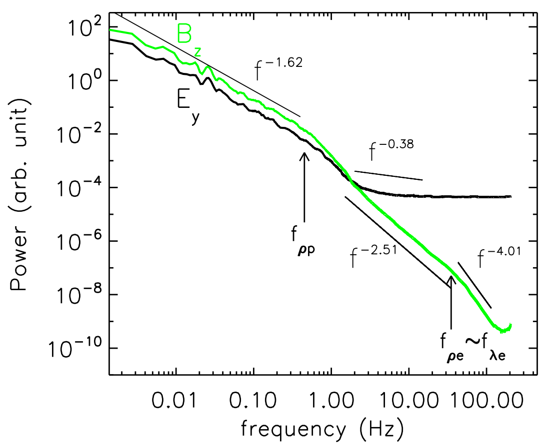

Fig. 4. Spectra of data from spacecraft 4 in the Despun System of reference (DS): E_y measured by EFW (bold black curve) and B_z measured by FGM and STAFF-SC merged at 1.5 Hz (green). The straight black lines are direct power law fits of the spectra. Vertical arrows are the Doppler-shifted proton and electron gyroradius and inertial lengths.

ment with these observations. KAW turbulence has been observed previously by [25,10], but only at large (proton) scales (up to 10 Hz). Here we are observing KAW behavior down to electron scales where enhanced dissipation becomes evident. This can be explained by electron Landau damping, as it is shown below.

To confirm this scenario of KAW energy cascade and dissipation, we have solved numerically the linear Maxwell–Vlasov equations assuming Maxwellian distributions of protons and electrons with characteristics that reflect the physical parameters deduced from the data. We assumed that the turbulence was quasi-two-dimensional (2D), i.e., $k_\parallel \ll k_\perp$. This assumption is justified by an analysis (not shown here) that used the k-filtering technique on the **k**-vectors distribution at large scales ($f < 10^{-2}$ Hz). That analysis confirmed the 2D nature at large scales. This 2D picture at large scales is likely to continue at the small scales as reported in previous studies [26,25]. Several previous observations have also reported the dominance of the 2D turbulence in the SW [24,27].

The results shown in Fig. 5 prove that under the plasma conditions observed here, KAW can propagate over a wide range of scales before being damped at the electron gyroscale [9,13]. The mode is shown to be only slightly damped at $k\rho_p \sim 1$ where $|\gamma|/\omega_r \sim 0.1$ (γ is the damping rate and ω_r is the real part of the frequency). The KAW mode is however strongly damped by electron Landau resonance at $k\rho_e \sim 1$ where $|\gamma|/\omega_r \sim 1$, which may explain the steepening of the magnetic spectrum to f^{-4} (here the resonance condition $\omega_r \sim k_\parallel V_{th_e}$ and the KAW dispersion relation $\omega_r = \pm k_\parallel V_A k_\perp \rho_p / \sqrt{\beta_p + 2/(1 + T_e/T_p)}$ [17] yield the dissipation scale $k\rho_e \sim 0.8$). We notice however that for moderate oblique propagation angles $\leqslant 80°$, scales $k\rho_p > 15$ are damped by proton Landau/cyclotron resonance ($\omega_r \sim \omega_{cp}$), which may yield proton heating.

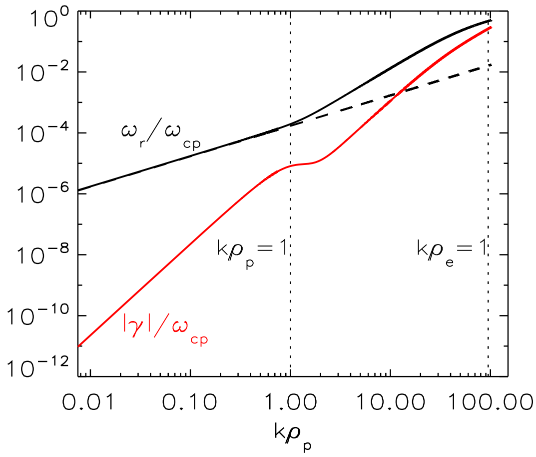

Fig. 5. Linear solutions of the Maxwell–Vlasov equations for $\theta = \arccos(\mathbf{k}, \mathbf{B}_0) = 89°$, obtained using the plasma parameters given in the text. The real part of the frequency (black) and the damping rate (red) are consistent with the kinetic Alfvén wave dispersion relation and damping [9,16]. The dashed line is the asymptote $\omega/\omega_{cp} = k_\parallel V_A/\omega_{cp}$. The plots stop at scales where $|\gamma| \sim \omega_r$.

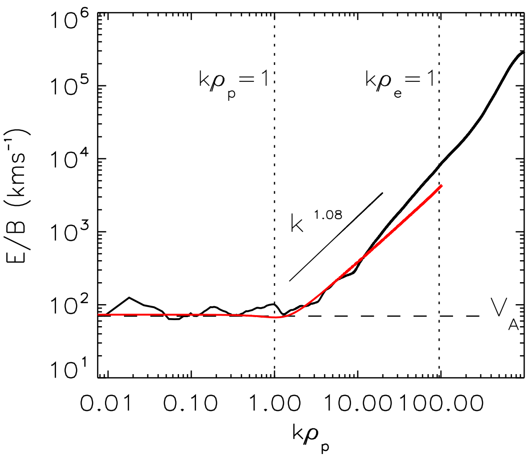

Fig. 6. The ratio E_y/B_z measured by Cluster 4 (black) compared to a similar ratio calculated from the linear Maxwell–Vlasov theory (red). The electric field data have been transformed into the plasma reference frame using the Lorentz transform $\mathbf{E}_{plas} = \mathbf{E}_{sat} - \mathbf{V} \times \mathbf{B}$ [10]. The horizontal dashed line is the Alfvén speed. The straight black line is a direct fit of E_y/B_z from $k\rho_p = 1.5$ to $k\rho_p = 20$. We used $\theta = \arccos(\mathbf{k}, \mathbf{v}) = 50°$ to transform frequency to $k\rho_p$.

Fig. 6 shows a comparison between the ratio of the electric to the magnetic field measured by Cluster and calculated from the linear kinetic theory of the KAW. There is very good agreement between theory and observations: (i) At large scales ($k\rho_p \leqslant 1$) the similar scaling $E^2 \sim B^2 \sim k^{-1.62}$ yields a constant ratio $V_\phi = E/B \sim V_A$, in agreement with the frozen-in flow approximation $\mathbf{E} = -\mathbf{V} \times \mathbf{B}$; (ii) At the scale $k\rho_p \geqslant 1$, dispersive effects set in yielding the linear scaling of the phase speed $V_\phi \sim k^{1.08}$, which also agrees with GK theory because $E^2/B^2 \sim k_\perp^2 \Rightarrow V_\phi \sim k_\perp$. We note finally that the departure from this linear scaling observed in Fig. 6 for $k\rho_p > 20$ is due to the noise in the electric field data that causes the flat E_y spectrum mentioned above. One would expect to observe a steepening of the E_y spectrum similar to B_z when the dissipation scale $k\rho_e \sim 1$ is reached [17].

4. Multi-spacecraft analysis of sub-proton scales using the *k*-filtering technique

The results shown above were obtained in a time interval where the Cluster spacecraft were separated by about 1000 km. These large spacecraft separation preclude using the *k*-filtering method to estimate the 3D wavenumber spectra and, consequently, investigate the nature of the small scale turbulence of interest here [4,22]. Therefore, we analyzed another data set where the spacecraft separation were about 100 km. The spectra of the magnetic turbulence are shown on Fig. 7.

We can see on Fig. 7 that the breakpoint at proton scales falls within the interval of frequencies $[f_{min}, f_{max}] = [0.04, 2]$ Hz accessible to analysis using the *k*-filtering [28–30,22]. Applying the *k*-filtering method on each frequency of this interval allowed us to obtain the 3D **k**-spectra of the turbulence, resolving therefore its anisotropy and nature at the corresponding scales (a more complete study of this interval will be published elsewhere).

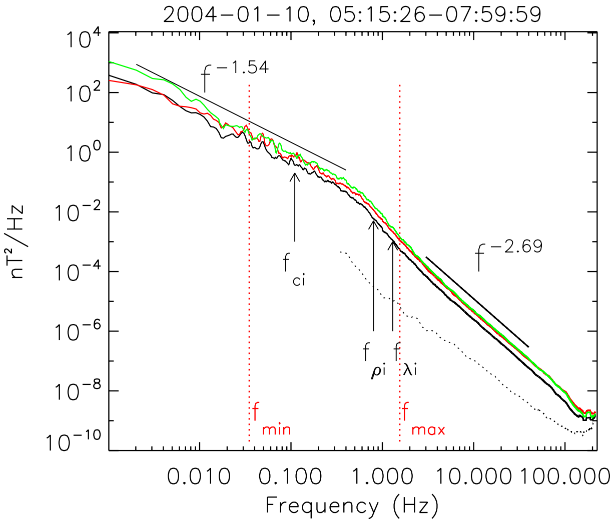

Fig. 7. Merged spectra from FGM ($f < 1.5$ Hz) and STAFF-SC data ($1.5 < f < 225$ Hz) in GSE on 2004-01-10 from 06h05 to 06h55. The vertical dotted lines (red) limit the range of frequencies accessible to analysis using the k-filtering [22]. The same description as in Fig. 2 applies to the rest of the figure.

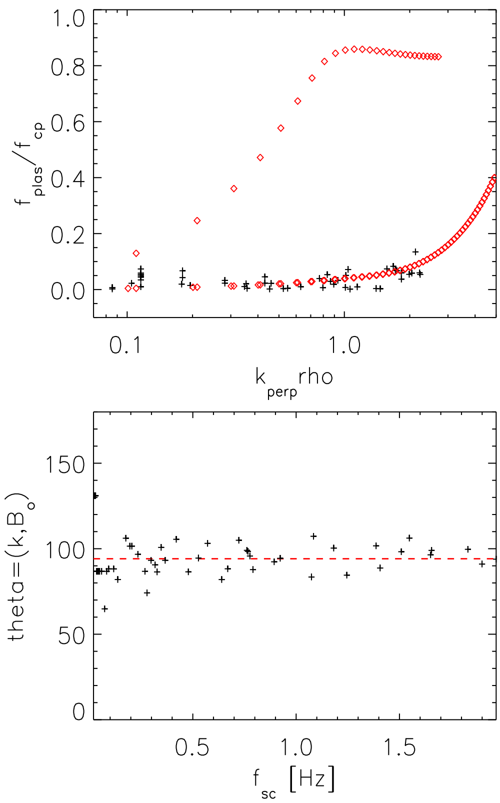

Fig. 8. Top: comparison of the experimental dispersion relations (crosses) to the theoretical ones as computed from the linear Vlasov theory (diamonds) for the average angle $\theta = \langle(\mathbf{k}, \mathbf{B}_0)\rangle \sim 86°$ (dashed line). Bottom: the angles between the local magnetic field and the $\mathbf{k}$-vectors of the turbulence estimated using the k-filtering technique for the interval of frequencies depicted on Fig. 7.

As shown in Fig. 8 (bottom), we found that the **k**-vectors of the turbulence lie nearly in the plane perpendicular to the mean magnetic field, with a mean angle $\theta = \langle(\mathbf{k}, \mathbf{B}_0)\rangle \sim 86°$. It is worth noting that this result is valid both below and above the proton gyroscale. This result validates the assumption used in [31] that large (proton) scale anisotropies "survive" at small (electron) scales. The top plot in Fig. 8 compares the experimental dispersion relations to the theoretical ones as computed from the linear Vlasov theory for the observed angle $\theta = \langle(\mathbf{k}, \mathbf{B}_0)\rangle \sim 86°$ and using the observed plasma parameters. This plot shows clearly that the turbulence is nearly stationary in the plasma rest frame ($f_{plas} \ll f_{cp}$) and follows the dispersion curve of the Alfvén mode $\omega \sim k_{\parallel} V_A$ up to the scale $k_{\perp}\rho \sim 2.5$. The observed experimental "dispersion" relations lie very far from the fast mode. Because larger **k**-vectors than the ones shown here are not accessible to measurements, we cannot conclude whether or not the nature of the turbulence at smaller scales (or higher frequencies) may change and follow the whistler mode. We will discuss in more detail this problem in a forthcoming paper.

5. Discussion and conclusions

We reviewed recent observations of cascade of the SW turbulence below the proton gyroscale and its dissipation at the electron gyroscale. We have shown that the kinetic theory of the highly oblique KAW turbulence can account for the observed cascade and dissipation. We found that collisionless electron Landau damping consistently explains the observations rather than proton cyclotron damping. These results were first obtained from mono-spacecraft analysis. Then they have been confirmed from direct multi-spacecraft measurements of the **k**-vectors of turbulence at sub-proton scales using the *k*-filtering method, when the Cluster separation were appropriate. This mechanism of cascade and dissipation at small scales may be applicable in other astrophysical contexts [7,16]. For example, in the solar corona, electron Landau damping, as observed here, may be an efficient mechanism for heating electrons. An open question remains however which is related to the physical conditions under which one would observe either scenarios: i) a dissipation-like spectra at the proton scale; ii) a continuous cascade below the proton scale and dissipation at the electron scale. This problem is currently being investigated.

References

[1] P. Escoubet, et al., The Cluster and Phoenix Missions, Kluwer Academic Publishers, Belgium, 1997.
[2] W.H. Matthaeus, M.L. Goldstein, Measurement of the rugged invariants of magnetohydrodynamic turbulence in the solar wind, J. Geophys. Res. 87 (1982) 6011–6028.
[3] Y. Narita, K.H. Glassmeier, F. Sahraoui, M.L. Goldstein, Wave-vector dependence of magnetic-turbulence spectra in the solar wind, Phys. Rev. Lett. 104 (2010) 171101.
[4] F. Sahraoui, G. Belmont, M.L. Goldstein, L. Rezeau, Limitations of multispacecraft data techniques in measuring wave number spectra of space plasma turbulence, J. Geophys. Res. 115 (2010) A04206, doi:10.1029/2009JA014724.
[5] M.L. Goldstein, M.D. Roberts, C. Fitch, Properties of the fluctuating magnetic helicity in the inertial and dissipation ranges of solar wind turbulence, J. Geophys. Res. 99 (1994) 11519–11538.
[6] R.J. Leamon, C.W. Smith, N.F. Ness, W.H. Matthaeus, H.K. Wong, Observational constraints on the dynamics of the interplanetary magnetic field dissipation range, J. Geophys. Res. 103 (1998) 4775–4787.
[7] R.J. Leamon, W.H. Matthaeus, C.W. Smith, G.P. Zank, D.J. Mullan, MHD-driven kinetic dissipation in the solar wind and corona, Astrophys. J. 537 (2000) 1054.
[8] O. Alexandrova, V. Carbone, P. Veltri, L. Sorriso-Valvo, Small-scale energy cascade of the solar wind turbulence, Astrophys. J. 674 (2008) 1153.
[9] O. Stawicki, S.P. Gary, H. Li, Solar wind magnetic fluctuation spectra: Dispersion versus damping, J. Geophys. Res. 106 (2001) 8273–8281.
[10] S.D. Bale, P.J. Kellogg, F.S. Mozer, T.S. Horbury, H. Rème, Observations of turbulence generated by magnetic reconnection, Phys. Rev. Lett. 94 (2005) 215002.
[11] D. Biskamp, E. Schwarz, A. Zeiler, A. Celani, J.F. Drake, Electron magnetohydrodynamic turbulence, Phys. Plasmas 6 (1999) 751.
[12] V. Krishan, S.M. Mahajan, Magnetic fluctuations and Hall magnetohydrodynamic turbulence in the solar wind, J. Geophys. Res. 109 (2004), doi:10.1029/2004JA010496.
[13] S.P. Gary, S. Saito, H. Li, Cascade of whistler turbulence: Particle-in-ell simulations, Geophys. Res. Lett. 35 (2008) L02104, doi:10.1029/2007GL032327.
[14] S. Galtier, von Kármán–Howarth equations for Hall magnetohydrodynamic flows, Phys. Rev. E 77 (2008) 015302.
[15] F. Sahraoui, S. Galtier, G. Belmont, On waves in incompressible Hall magnetohydrodynamics, J. Plasmas Phys. 73 (2007) 723–730.
[16] A.A. Schekochihin, S.C. Cowley, W. Dorland, G.W. Hammett, G.G. Howes, E. Quataert, T. Tatsuno, Astrophysical gyrokinetics: kinetic and fluid turbulent cascades in magnetized weakly collisional plasmas, Astrophys. J. Suppl. 182 (2009) 310–377.
[17] G.G. Howes, W. Dorland, S.C. Cowley, G.W. Hammett, E. Quataert, A.A. Schekochihin, T. Tatsuno, Kinetic simulations of magnetized turbulence in astrophysical plasmas, Phys. Rev. Lett. 100 (2008) 065004.
[18] A. Balogh, C.M. Carr, M.H. Acuna, M.W. Dunlop, T.J. Beek, P. Brown, K.-H. Fornacon, E. Georgescu, K.-H. Glassmeier, J. Harris, G. Musmann, T. Oddy, K. Schwingenschuh, The cluster magnetic field investigation: overview of in-flight performance and initial results, Ann. Geophys. 19 (2001) 1207–1217.
[19] N. Cornilleau-Wehrlin, G. Chanteur, S. Perraut, L. Rezeau, P. Robert, A. Roux, C. de Villedary, P. Canu, M. Maksimovic, Y. de Conchy, D. Hubert, C. Lacombe, F. Lefeuvre, M. Parrot, J.L. Pinçon, P.M.E. Dçcrçau, C.C. Harvey, Ph. Louarn, O. Santolik, H.St.C. Alleyne, M. Roth, T. Chust, O. Le Contel, STAFF team, First results obtained by the Cluster STAFF experiment, Ann. Geophys. 21 (2003) 437–456.
[20] G. Gustafsson, M. André, T. Carozzi, A.I. Eriksson, C.-G. Fälthammar, R. Grard, G. Holmgren, J.A. Holtet, N. Ivchenko, T. Karlsson, Y. Khotyaintsev, S. Klimov, H. Laakso, P.-A. Lindqvist, B. Lybekk, G. Marklund, F. Mozer, K. Mursula, A. Pedersen, B. Popielawska, S. Savin, K. Stasiewicz, P. Tanskanen, A. Vaivads, J.-E. Wahlund, First results of electric field and density observations by Cluster EFW based on initial months of operation, Ann. Geophys. 19 (2001) 1241–1258.
[21] R.J. Leamon, C.W. Smith, N.F. Ness, Dissipation range dynamics: Kinetic Alfvén waves and the importance of β_e, J. Geophys. Res. 104 (1999) 22331.
[22] F. Sahraoui, M.L. Goldstein, G. Belmont, A. Roux, L. Rezeau, P. Canu, P. Robert, N. Cornilleau-Wehrlin, O. Lecontel, T.D. De Wit, J.L. Pincon, K. Kiyani, Multi-spacecraft investigation of space turbulence: Lessons from Cluster and input to the Cross-Scale mission, Planet. Space Sci. (2010), doi:10.1016/j.pss.2010.06.001.
[23] O. Alexandrova, J. Saur, C. Lacombe, A. Mangeney, J. Mitchell, S.J. Schwartz, P. Robert, Universality of solar-wind turbulent spectrum from MHD to electron scales, Phys. Rev. Lett. 103 (2009) 165003.
[24] W.H. Matthaeus, M.L. Goldstein, D.A. Roberts, Evidence for the presence of quasi-two-dimensional nearly incompressible fluctuations in the solar wind, J. Geophys. Res. 95 (1990) 20673–20683.
[25] B. Grison, F. Sahraoui, B. Lavraud, T. Chust, N. Cornilleau-Wehrlin, H. Rème, A. Balogh, M. André, Wave particle interactions in the high-altitude polar cusp: a Cluster case study, Ann. Geophys. 23 (2005) 3699–3713.
[26] F. Sahraoui, G. Belmont, L. Rezeau, N. Cornilleau-Wehrlin, J.L. Pinçon, A. Balogh, Anisotropic turbulent spectra in the terrestrial magnetosheath as seen by the cluster spacecraft, Phys. Rev. Lett. 96 (2006) 075002.
[27] K.T. Osman, T.S. Horbury, Multispacecraft measurement of anisotropic correlation functions in solar wind turbulence, Astrophys. J. 654 (2007) L103.

[28] J.L. Pinçon, F. Lefeuvre, Local characterization of homogeneous turbulence in a space plasma from simultaneous measurements of field components at several points in space, J. Geophys. Res. 96 (1991) 1789–1802.
[29] F. Sahraoui, J.L. Pinçon, G. Belmont, L. Rezeau, N. Cornilleau-Wehrlin, P. Robert, L. Mellul, J.M. Bosqued, A. Balogh, P. Canu, G. Chanteur, ULF wave identification in the magnetosheath: The *k*-filtering technique applied to Cluster II data, J. Geophys. Res. 108 (2003) 1335–1354.
[30] F. Sahraoui, G. Belmont, J.L. Pinçon, L. Rezeau, A. Balogh, P. Robert, N. Cornilleau-Wehrlin, Magnetic turbulent spectra in the magnetosheath: new insights, Ann. Geophys. 22 (2004) 2283–2288.
[31] F. Sahraoui, M.L. Goldstein, P. Robert, Y.V. Khotyaintsev, Evidence of a cascade and dissipation of solar-wind turbulence at the electron gyroscale, Phys. Rev. Lett. 102 (2009) 231102.